Canadian Science Publishing | Canadian Journal of Forest Research

Foliar sampling with a UAS reveals spectral and functional trait differences within tree crowns

Journal:	*Canadian Journal of Forest Research*
Manuscript ID	cjfr-2019-0452.R1
Manuscript Type:	Article
Date Submitted by the Author:	29-May-2020
Complete List of Authors:	Schweiger, Anna Katharina; Université de Montréal, Institut de recherche en biologie végétale; Université de Montréal, Département de sciences biologiques Lussier Desbiens, Alexis; Université de Sherbrooke, Createk Lab Charron, Guillaume; Université de Sherbrooke, Createk Lab La Vigne, Hughes; Université de Sherbrooke, Createk Lab Laliberté, Etienne; Université de Montréal, Institut de recherche en biologie végétale; Université de Montréal, Département de sciences biologiques
Keyword:	functional trait mapping, spectroscopy, twig sampling, Unmanned Aerial System, Unmanned Aerial Vehicle
Is the invited manuscript for consideration in a Special Issue? :	Unmanned Aerial Vehicles in Forest Science and Management

Foliar sampling with a UAS reveals spectral and functional trait differences within tree crowns

Anna Katharina Schweiger[1,2,*], Alexis Lussier Desbiens[3], Guillaume Charron[3], Hughes La Vigne[3], Etienne Laliberté[1,2]

[1] Institut de recherche en biologie végétale, Université de Montréal, 4101 Sherbrooke Est, Montréal, QC H1X 2B2, Canada

[2] Département de sciences biologiques, Université de Montréal, C. P. 6128, Succursale Centre-ville, Montréal, QC H3C 3J7, Canada

[3] Createk Lab, Université de Sherbrooke, Parc Innovation - ACELP, Pavillon P2 3000 Boul. de l'Université, Sherbrooke, QC J1K 0A5, Canada

* Corresponding author

Email addresses:

AKS: anna.k.schweiger@gmail.com

ALD: Alexis.Lussier.Desbiens@USherbrooke.ca

GC: guillaume.charron2@usherbrooke.ca

HLV: hughes.la.vigne@usherbrooke.ca

EL: etienne.laliberte@umontreal.ca

Abstract

Imaging spectroscopy is currently the best approach for continuously mapping forest canopy traits, which is important for ecosystem and biodiversity assessments. Ideally, models are trained with trait data from fully sunlit top-of-canopy leaves. However, sampling top-of-canopy leaves is often difficult and sunlit foliage from the crown periphery is collected instead, assuming minimal within-crown trait variation among sunlit leaves. We tested the degree to which crown position affects foliar traits and spectra using mixed-effects models comparing sun leaves from crown centres of mature *Acer saccharum* trees collected with DeLeaves, a novel twig-sampling Unmanned Aerial System device, to sun leaves from the crown periphery collected with a pole pruner. Sun leaves from the crown centre differed from sun leaves from the crown periphery in absorption, reflectance and transmittance, and in a series of foliar traits, including leaf thickness, leaf mass and leaf nitrogen content per unit area, pointing out differences in resource allocation depending on sun exposure. Our study highlights the importance of matching exactly the location of foliar samples and spectral data, and of sampling across gradients of intra-individual variation for accurately predicting foliar trait distributions across and within canopies with imaging spectroscopy.

Keywords

functional trait mapping, spectroscopy, twig sampling, Unmanned Aerial System, Unmanned Aerial Vehicle

Introduction

Recent technological advances in remote sensing, including imaging spectroscopy, provide ecologists with the unique ability to monitor the diversity and function of forests continuously over large regions. In addition, the "ecological data revolution" provides researchers and forest managers with an increasing amount of open access organismal and remote sensing data, and with tools kits for processing and interpreting these data (Bush et al. 2017). Large-scale research initiatives, such as the National Ecological Observatory Network (NEON, www.neonscience.org), are making their protocols and databases, containing foliar trait, community composition, and high resolution remote sensing data, publicly available. In addition, space agencies are currently investing in new instrument fleets for Earth observation, including imaging spectrometers allowing to remotely sense forest canopy traits repeatedly worldwide (Stavros et al. 2017). Together with ground observation data, these instruments will enable assessing the status of ecosystems and biodiversity at unprecedented detail (Turner 2014). This commitment to monitoring planet Earth comes at a critical time as global losses in plant species (Humphreys et al. 2019) and deforestation (Curtis et al. 2018) are putting ecosystem functions and services at risk.

Functional trait ecology is the most promising approach for scaling biological interaction across scales, and for modelling, predicting, and mitigating the effects of global change on ecosystem function and services (Laughlin 2014; Lavorel and Garnier 2002; Shipley et al. 2016; Violle et al. 2014). Plant functional traits are any characteristics that have a potentially significant influence on an individual's establishment, survival, and fitness. At the individual scale, plant functional traits reveal trade-offs among a plant's investment into different organs

(Osnas et al. 2013; Reich et al. 1997; Wright et al. 2004). At the community scale, investigating plant functional traits and trait syndromes, collections of interrelated traits, provide insight into resource partitioning and community assembly (Hart et al. 2016; McGill et al. 2006). And at landscape and continental scales, incorporating plant functional traits improves predictions of water and energy fluxes among atmosphere, biosphere, and geosphere in Earth System Models (Rockström et al. 2009; Rogers et al. 2017), and can also guide large-scale conservation planning (Asner et al. 2017). However, large inter- and intraspecific variation in plant functional traits imposes difficulties on their integration in large-scale ecosystem studies (Serbin et al. 2019). Measuring the traits of individual plants is laborious and it is logistically impossible to measure a wide range of traits over large spatial extents (Ustin et al. 2004) with traditional field techniques (see e.g. Perez-Harguindeguy et al. 2013). Remote sensing, particularly imaging spectroscopy and light detection and ranging (Lidar), provide the only practical means for mapping continuously and repeatedly the spatial distribution of chemical and structural plant traits (Jetz et al. 2016; Schimel et al. 2013; Turner 2014), from which plant community types, plant functional types and, in some cases, taxonomic groups can be inferred (for reviews see Fassnacht et al. 2016; Wang and Gamon 2019).

Spectroscopy is the study of the interaction between electromagnetic energy and matter, and has a long history in detecting and quantifying chemical compounds in chemometrics (Martens 2001; Wold et al. 1983) and planetary sciences (Schaepman et al. 2009). Light absorption and scattering depend on the chemical composition and structural characteristics of the material measured. Spectrometers measure the interaction of light and matter in dozens of narrow wavelength channels, covering the visible (VIS, 400–700 nm), near- (NIR, 700–1000 nm) and shortwave-infrared (SWIR, 1000–2500 nm) regions of the electromagnetic spectrum.

Spectral profiles of plants (i.e., the curves resulting from spectral measurements at short wavelength intervals) depend on a range of leaf and whole-plant traits (Gates et al. 1965; Knipling 1970), including pigment composition, micro- and macronutrient content, water content, specific leaf area (SLA), surface and internal structure of leaves, and canopy architecture (see e.g., Curran 1989; Curran et al. 2001; Ollinger 2011; Slaton et al. 2001; Ustin et al. 2009). Spectral profiles thus capture key differences in foliar chemistry, morphology, life history strategies, and responses to environmental variation, which have evolved over time and reflect ecological strategies (Cavender-Bares et al. 2017; Ustin and Gamon 2010). Ecological applications of imaging spectroscopy include mapping of functional traits (e.g., Asner et al. 2011; Singh et al. 2015; Wang et al. 2019); the differentiation of plant communities (e.g., Foster and Townsend 2004; Schweiger et al. 2017), species (e.g. Asner and Martin 2008; Clark et al. 2005; Lopatin et al. 2017), and genotypes (e.g., Madritch et al. 2014); the detection of disease (Herrmann et al. 2018; e.g., Pontius et al. 2005) and stress symptoms (e.g., Asner et al. 2016; Singh et al. 2016); and the estimation of other dimensions of plant biodiversity based on spectral diversity (e.g., Draper et al. 2019; Féret and Asner 2014; Laliberté et al. 2019; Palmer et al. 2002; Rocchini et al. 2010; Schweiger et al. 2018; Wang et al. 2018). Imaging spectrometers are regularly mounted on airplanes, including NASA's AVIRIS (Green et al. 1998) and ESA's APEX (Schaepman et al. 2015) instruments, and experimental platforms, including mobile and stationary tram systems (Gamon et al. 2006), and flux towers (Gamon 2015). Current frontiers in imaging spectroscopy include the development of UAS's (Aasen et al. 2018; Arroyo-Mora et al. 2019) and upcoming spaceborne missions, such as ESA's EnMAP (Guanter et al. 2015), JAXA's HISUI (Iwasaki et al. 2011), and NASA's SGB (National Academies of Sciences and Medicine 2018) missions.

Spectra of plants can be measured on dried and ground leaf material (e.g., (Curran et al. 2001; Kokaly and Clark 1999), on fresh leaf samples (e.g., Gates et al. 1965), and estimated from spectral images (e.g., Green et al. 1998). Partial least squares regression (PLSR, Wold et al. 1983) is one the most popular statistical methods for modelling and predicting continuous information from high dimensional data, such as spectra. Developed in the 1970's and 1980's for laboratory spectroscopy (Martens 2001), PLS methods were specifically designed to deal with the high degree of autocorrelation inherent in spectral data. For training a model with PLS, spectra (the predictors or x variables) are being matched to continuous data (the outcomes or y variables). For example, for functional trait mapping in forests, where harvesting all foliage within a given area is usually impossible, the biological outcome variables can be determined from leaf samples that are representative for the tree or trees present within a certain number of pixels captured by the sensor. Generally it is expected that the centre pixel or pixels of tree crowns dominate the spectral signal captured by airborne sensors with spatial resolutions at the m-scale, and they also often have the best illumination. Thus, methodological guidelines in imaging spectroscopy (see e.g., https://www.neonscience.org/data-collection/protocols-standardized-methods) suggest sampling fully sunlit and mature leaves from the top of the canopy. However, the very top of a tree (i.e., the crown summit) is not always reachable with standard sampling equipment, such as pole pruners or line launchers. Canopy tops might be out of reach even for professional tree climbers that can operate equipment from within the crown; and more permanent infrastructure, such as canopy cranes, are difficult to deploy and expensive (Charron et al. 2020). In addition, the degree to which the chemical and structural composition of sunlit leaves from the top and centre of tree crowns are representative for the entire canopy is not clear.

Leaf structure and function within canopies vary depending on gradients of light, microclimate, and the degrees of herbivory and pathogen pressure (Niinemets 2007). Particularly well studied are anatomical and biochemical differences among sun and shade leaves which determine, for example, their maximum photosynthesis rates and longevity (Lichtenthaler et al. 1981; Niinemets 2007; Valladares and Niinemets 2008). At high light sun leaves photosynthesize more and reach light saturation more gradually and at higher irradiance than shade leaves, while at low light shade leaves can exceed the maximum photosynthesis rates of sun leaves (Lichtenthaler et al. 1981). Generally, higher photosynthetic rates are associated with sun leaves being thicker than shade leaves, which is mainly achieved by longer palisade parenchyma cells increasing the space per unit area available for chloroplasts (Lichtenthaler et al. 1981; Niinemets 2007). In addition, sun leaves often have a more robust cuticle reducing water loss and increasing specular reflectance at high irradiance. Shade leaves are generally thinner than sun leaves and have proportionally more spongy mesophyll cells (Lichtenthaler et al. 1981), which increases path length through light scattering within leaves increasing the probability of photon absorption by chlorophyll. Although shade leaves have compared to sun leaves often less chloroplasts per unit area, they can have higher chlorophyll concentrations per chloroplast resulting in relatively similar chlorophyll concentrations per unit mass (Vogelman et al. 1996). Comparative studies tend to describe differences among sun and shade leaves as extreme cases, but it is clear that these represent the tails of the distribution of traits along more complex light gradients within tree crowns (Ellsworth and Reich 1993; Gamon and Berry 2012; Niinemets 2007; Shipley et al. 2005; Valladares and Niinemets 2008).

Several studies have highlighted the importance of incorporating intra- and interspecific variation for trait predictions from spectral images (Serbin et al. 2019; Singh et al. 2015), but intra-individual variation in foliar traits within the outer tree crown surface has not received much attention. Here we took advantage of a custom UAS for foliar sampling to collect leaves from the centre and top of tree crowns which are difficult to reach with standard sampling methods. We tested for differences in chemical and structural leaf traits and spectra between paired samples of sunlit, mature and healthy leaves of ten sugar maple (*Acer saccharum* Marshall) trees, one set from crown periphery collected with a pole pruner, the other set from the top and centre of the crown collected with the UAS. We hypothesized that crown position would influence leaf traits and spectral only marginally, such that samples collected with the pole pruner would be representative for top of the canopy leaves.

Materials and methods

On 26 June 2019 we sampled sunlit leaves of ten sugar maple trees near Sherbrooke (45.582, -71.875) in Southern Québec (Supplementary Fig.1) under dry and sunny conditions, with minimal wind. The study site is located within the sugar maple-basswood bioclimatic domain, and has a mean annual air temperature and precipitation of 5.1ºC and 1287 mm, respectively. The stands are dominated by sugar maple with some red maple (*Acer rubrum* L.), American beech (*Fagus grandifolia* Ehrh.) and yellow birch (*Betula alleghaniensis* Britton). The soils are typically Orthic Humo-Ferric and Ferro-Humic Podzols characterized by a sandy loam to loam texture and a moder type forest floor varying in depth from 5 to 10 cm.

We collected two twigs from each tree crown, one from the side of the crown with a pole pruner (Fig. 1A), and one from the top and centre of the crown using the DeLeaves Forestry edition twig-sampling tool (DeLeaves, Sherbrooke, www.deleaves-drone.com; Charron et al. 2020) operated from an off-the-shelf Unmanned Aerial Vehicle (UAV; here a Tarot 680 Pro Hexacopter; Fig. 1B). The DeLeaves sampling device consists of a grasping mechanism, a rotating saw, a branch holding mechanism and a camera installed on a carbon fibre rod, and a custom quick release system under the drone. It has a total weight of 1100 g and can be operated from any UAV with a maximum payload allowance of 1500 g (for details see Charron et al. 2020)

After collection the twigs were immediately sealed into plastic bags, cooled and measured as soon as possible. We measured spectral reflectance and transmittance of six healthy and undamaged leaves per twig using a portable field spectrometer (SVC HR-1024i plus software; Spectra Vista Corporation, Poughkeepsie, NY) covering the wavelength range of 340 to 2,500 nm in 1,024 spectral bands, fitted with an integrating sphere (DC-R/T, Spectra Vista Corporation, Poughkeepsie, NY) following the standardized leaf sampling protocol developed by the Canadian Airborne Biodiversity Observatory (CABO; Laliberté and Soffer 2018). Spectral processing followed the CABO spectral processing protocol (Schweiger and Laliberté 2019) and included correcting artefacts at the sensor overlap regions (around 900 nm and 1,900 nm, respectively), resampling to 1 nm spectral resolution, removing noisy regions at the beginning and end of the spectrum (centre wavelengths smaller than 400 nm or greater than 2,400 nm), and applying a Savitzky-Golay filter to reduce sensor noise. We calculated absolute leaf reflectance (%), transmittance (%), and absorptance (%; absorptance = 1 - reflectance - transmittance) per leaf (see Laliberté and Soffer 2018), and averaged the values of six leaves per twig.

From each twig we collected a bulk leaf sample for foliar trait analysis. Leaves were weighed in the field to determine leaf fresh mass (LFM, g), rehydrated for 6 h, weighed to determine rehydrated leaf mass (RLM, g) and scanned for total leaf area (LA, cm^2). Then leaves were oven-dried for 72 h and weighed again to determine dry mass (LDM, g). Based on these measurement we calculated leaf mass per area (LMA, g m^{-2}) as LMA = LDM x LA^{-1} x 10^{-4}, equivalent water thickness (EWT, µm) as EWT = (LFM - LDM) x LA^{-1} x 10^4, relative water content (RWC, %) as RWC = [(LFM - LDM) ÷ (RLM - LDM)] × 100, leaf dry matter content (LDMC, mg g^{-1}) as LDMC = LDM × RLM^{-1} x 10^3, leaf water content (LWC, %) as LWC = 1 - LDMC (for details see Laliberté 2018), and leaf thickness (LT, µm) as LT = LMA x $LDMC^{-1}$ x 10^4 (Vile et al. 2005). Leaf carbon (C, %) and nitrogen content on a mass basis (N, %) were determined from oven-dried and ground samples using an elemental analyzer (CHNOS Elemental Analyzer Vario Micro Select; Elementar Analysesysteme GmbH, Hanau, Germany; see Ayotte et al. 2019). The concentrations on a mass basis (%) of carbon fractions, including non-structural carbohydrates (NSC), hemicellulose, cellulose, and lignin, were determined from oven-dried and ground samples using sequential digestion (Fiber Analyzer 2000; ANKOM Technology, Macedon, NY; see Ayotte and Laliberté 2019). The contents of C, N, and fibre fractions on an area basis (mg m^{-2}) were calculated as the product of LMA and the respective contents on a mass basis.

We tested the hypothesis that sun leaves from the top of the crown (sampled with the UAS) differed from sun leaves from the side of the crown (sampled with the pole pruner) regarding their foliar traits, and band-wise reflectance, transmittance, and absorptance using linear mixed-effects (LME) models with “tree identity” as the random factor. Since p-values are uninformative in LME’s, we used a likelihood ratio (LR) > 4 as the threshold indicating an effect of sampling position on leaf traits and spectra, meaning that it would be least four times more likely that leaves differ in their foliar traits and spectra depending on sampling position (M1) than that they are the same (M0). We used R (R Core Team 2019) and the lme4 package (Bates et al. 2014) for all analyses.

Results

Foliar traits

We found evidence for intra-individual differences in a series of leaf traits depending on crown position (Table 1). Sun leaves sampled from the top and centre of the crown with the UAS had greater LMA than sun leaves from the crown periphery sampled with the pole pruner (LR = 14.3, $P < 0.001$; Fig. 2A). This difference was likely driven by an increase in leaf thickness (LR = 14.4, $P < 0.001$; Fig. 2B) and not leaf density, which is strongly correlated with LDMC (LR = 0.6, P = 0.44; see Vile et al. 2005). Because of the difference in leaf thickness, leaves from the top and centre of the crown also had on an area basis (g m^{-2}) higher contents of N (LR = 14.9, $P < 0.001$; Fig. 2C), as well as C (LR = 13.2, $P < 0.001$), NSC (LR = 14.2, $P < 0.001$), cellulose (LR = 8.7, P = 0.003), and lignin (LR = 13.3, $P < 0.001$; Supplementary Fig. 2) than leaves from the side of the crown. We found no differences in chemical traits between leaves from the top and from the side of the crown when traits were expressed on a mass basis (%), except for cellulose content which was lower in leaves from the crown centre (LR = 9.7, P = 0.002; Fig. 2F). Further, compared to leaves from the crown periphery, leaves from the crown centre had higher EWT (LR = 10.9, P = 0.001; Fig. 2D), representing the amount of water at the time measurement (i.e., the depth of the water column as we cross the leaf), but lower RWC (LR =

9.9, P = 0.002; Fig. 2E), representing the amount of water at the time of measurement relative to a fully hydrated leaf.

Spectral properties

Several wavelength regions differed between sun leaves from the top of the crown and sun leaves from the crown periphery. Leaves from the top of the crown absorbed more light in the green, between ~510 and 570 nm, at the red edge, between ~710 and 750 nm, and across the entire SWIR, at wavelength greater than ~1140 nm, than leaves from the crown periphery (Fig. 3A). Greater SWIR absorption by leaves from the top of the crown compared to leaves from the crown periphery, including at the two major water absorption features at ~1450 and 1950 nm, led to less forward- (i.e., transmittance) and back-scattering (i.e., reflectance) in this wavelength region (Fig. 3B). Further, leaves from the top of the crown transmitted less light in the blue, between ~400 and 450 nm, in the green, between ~500 and 600 nm, and in the NIR regions of the spectrum compared to leaves from the crown periphery (Fig. 3B top). In addition, leaves from the top of the crown compared to leaves from the crown periphery reflected more light in the blue, between ~400 and 500 nm, and red, between ~650 and 700 nm, wavelength regions (Fig 3B bottom).

Discussion

Tree crowns are complex systems within which resource allocation is influenced by three-dimensional gradients of light, microclimate, herbivory, and pathogen pressure. We focus our discussion on the interaction of light with leaves, as light is together with nutrients, water and carbon dioxide (CO_2) a primary resource for plants. Light gradients occur throughout the canopy, and, although we did not measure radiation rates or the duration of leaves' sun exposure depending on crown position, it is likely that leaves from the side of the crown received less intense sunlight for fewer hours than leaves from the top of the crown. We found that many regions of the spectrum (Fig. 3) and a number of leaf traits, including LMA, leaf thickness, EWT, RWC, the contents of C, N, NSC, cellulose, and lignin on an area basis, and cellulose on a mass basis (Table 1) varied significantly with sampling position. Our results are consistent with existing knowledge about the influence of light gradients on leaf structure and biochemistry (Lichtenthaler et al. 1981; Niinemets 2007; Shipley et al. 2005). However, the differences in leaf traits and spectra between sunlit foliage from the top compared to the side of the crown were greater than we expected, given that all leaves were collected from the outer crown layer and thus can be classified as sun leaves. On a light gradient ranging from maximum sun exposure during daylight hours to full shade, leaves from the top of the crown resembled leaves experiencing maximum sun exposure in form and function, while leaves from the crown periphery resembled leaves receiving less light. This has important implications for imaging spectroscopy and for models predicting foliar traits from spectra.

The increase in LMA and leaf thickness with crown centrality is likely to be explained by the tendency of palisade cell length and number of palisade cell layers to increase with increasing sun exposure (Lichtenthaler et al. 1981). Longer palisade cells and more palisade cell layers tend to contain more chloroplasts per unit area, within which Ribulose-1,5-bisphosphate carboxylase/oxygenase (Rubisco) fixes CO_2. Rubisco contains about 20–30 % of total leaf N in C3 plants (Evans and Seemann 1989), and leaves in high light environments tend to have more Rubisco leading to greater content of leaf N per unit area in thicker leaves (Niinemets 2007). Notably, leaf N on a mass basis did not change with sampling position, probably because thinner leaves with fewer chloroplasts tend to contain more chlorophyll per chloroplast (Niinemets 2007). Similarly, leaves from the top of the canopy had higher amounts of carbon related traits on an area basis (Table 1, Supplementary Fig. 2), highlighting that changes in areas based measurements in leaf chemistry arise largely through scaling with LMA (Ellsworth and Reich 1993). Cellulose content was the only leaf trait included in our study that varied significantly on a mass basis between leaves from the crown centre and crown periphery. Although we did not specifically investigate leaf anatomy, we explain this by thinner leaves from the crown periphery likely having proportionally more vascular tissue, relative to mesophyll, with thicker cell walls than the thicker leaves from the crown centre. Although, leaves from the crown centre had higher EWT, indicating greater leaf water content at the time of measurement, than leaves from the crown periphery, leaves from the crown centre were less turgescent, indicated by a lower RWC, expressing leaf water content at the time of measurement relative to leaf water content of a fully hydrated leaf. This was likely caused by a greater degree of sun exposure of the crown centre compared to the crown periphery, which led to more water loss through transpiration during the morning hours preceding our measurements. Sampling position affected all chemical leaf traits (the contents of C, N, NSC, cellulose, and lignin), except for hemicellulose content, expressed on an area basis, while it affected only one leaf trait expressed on a mass basis (cellulose content), pointing out that area and mass based trait measurements describe fundamentally different trade-offs. Generally, area based measurements more adequately describe physiological processes and leaf anatomy, while mass based measurements better describe allocation patterns and energy budgets.

Leaf water content strongly influences leaf spectral properties throughout the SWIR (Curran 1989; Knipling 1970; Ollinger 2011). Water causes not only distinct absorption features at 1450 nm and 1950 nm, and smaller features in the NIR-SWIR transition region at 980 nm and 1150 nm, but also generally high absorption beyond 1400 nm due to rotational-vibrational properties of water molecules (Ollinger 2011). The increased SWIR absorption, and decreased transmittance and reflectance of leaves from the top of the crown compared to leaves from the crown periphery can be explained by their greater water content at the time of measurement (EWT). Leaves from the centre of the crown compare to leaves from the crown periphery also likely had more cell-to-air interfaces per unit area (Slaton et al. 2001), which probably led to increased forward-scattering (i.e., reflectance) in the NIR (at the expense of transmittance), since differences in density between air and water lead to refraction (Ollinger 2011). Leaves from centre of the crown compared to leaves from the side of the crown absorbed more light in the green, but reflected more (and transmitted less) in the red and blue regions of the spectrum, which is likely associated with differences in pool sizes of photoprotective carotenoid pigments relative to chlorophyll (Gamon and Berry 2012). We used the photochemical reflectance index (PRI, Gamon et al. 1992) to compare our leaf samples. Generally, lower PRI values [calculated as PRI = (reflectance at 531 nm - reflectance at 570 nm) / (reflectance at 531 nm + reflectance at 570 nm)] are associated with higher carotenoid to chlorophyll ratio, lower epoxidation state of xanthophyll cycle pigments which dissipate excess absorbed photosynthetically active radiation as heat (Demmig-Adams and Adams 1996), and lower light use efficiency (Gamon et al. 1992). Therefore, PRI and changes in PRI capture short term responses to excess light (xanthophyll pigment conversion) as well as long term changes in pigment pool sizes due to leaf development, leaf age, sun exposure, and chronic stress (Gamon et al. 1992; Gamon and Berry 2012). Most leaves from the centre of the crown had lower PRI values than leaves from the crown periphery (Supplementary Fig. 3). Given the time it takes to collect foliar samples and measure them, it is likely that the PRI signal was primarily driven by differences in pigment pool size and not xanthophyll cycle activity. Thus, our result points towards sun leaves from the centre of the crown investing more in carotenoid pigments relative to chlorophylls, as they likely experience increased sun exposure compared to sun leaves from the crown periphery.

The UAS twig sampling device offered the only possibility for us to collect leaves from the top of crown of our maple trees within a reasonable amount of time (the average time for sample collection was ~5 min). It would have been difficult for professionals to climb high enough for reaching the top of the crowns with a pole pruner because tree branches were relatively thin. Likewise, reaching the top of the tree with a line launcher (Youngentob et al. 2016) would have been difficult because of the high density of foliage, and using a canopy crane was not an option due to the high cost and limited accessibility of the site. Pole pruners are easy to use and inexpensive and are thus regularly used for twig sampling, including the collection of foliar samples for remote sensing studies. Generally, it is assumed that healthy, mature, sunlit leaves collected more towards the side of the crown are representative of the leaves from the crown centre. However, our results show that this assumption can introduce bias for remote sensing of foliar traits in forests. Combining imaging spectroscopy data collected at the m-level from airplanes with trait data sampled from the same crowns is the current gold standard for continuous trait mapping in forest ecosystems (Asner et al. 2017; Asner et al. 2011; Serbin et al. 2019; Singh et al. 2015). Although the careful matching of leaf samples and spectra has been emphasized and possibilities for incorporating intra-individual trait variation at the vertical level in trait mapping has been explored (Singh et al. 2015), less attention has been paid to intra-individual variation at the outer layer of leaves in the crown. More studies are needed to quantify the degree to which different parts of the canopy contribute to remotely sensed signals. Our results suggest that remote sensing products, such as trait maps, could be improved by incorporating intra-individual variation of foliar characteristics, for example by sampling leaves from multiple position throughout the top layer of the crown. Focusing on the centre of the crown with UAS precision sampling provides another option and could be combined with tree segmentation algorithms allowing the automatic extraction of image pixels from crown centres (e.g., Maschler et al. 2018). Looking ahead, trait mapping from spectral imagery acquired by satellites would likely also benefit from incorporating intra-individual variation during the upscaling process. In addition, imaging spectroscopy from UASs, an active area of research (Arroyo-Mora et al. 2019), will provide exciting opportunities for studying the functional complexity of tree crowns at the cm level. Matching spectra exactly to the positions of foliar sample collection will be important for such high spatial resolution remote sensing studies.

In summary, our study highlights the importance of matching accurately leaves and spectra during spectroscopic field campaigns. Twig sampling devices operated from UAS's provide a valuable, cost- and time-effective option for sampling from the top and centre of tree crowns (Charron et al. 2020), which are difficult to reach with conventional sampling methods. Opportunities for imaging spectroscopy across scales are rapidly increasing (Turner 2014). Thus far, imaging spectrometers have been mostly operated from airplanes at relatively high costs. Upcoming satellite missions will collect spectral images of Earth repeatedly across large spatial extents, while UAS imaging spectroscopy will allow investigating resource allocation in forests at the cm level. Foliar traits express specific adaptations of leaves for optimizing resource allocation within the complex light environment of a crown, including trade-offs in photosynthesis, photoprotection, and longevity. Incorporating intra-individual foliar variation can be expected to improve the accuracy of remote sensing products, which are becoming increasingly important for predicting energy and water fluxes, and for global biodiversity assessments.

Acknowledgements

We thank Florence Blanchard, Sabrina Demers-Thibeault, Alexandra Massey, Antoine Mathieu and Maria Juliana Pardo for field sampling, and Isabelle Gareau and Sabrina Demers-Thibeault for laboratory analysis. Thanks to John A. Gamon for comments on the results. This research is part of the Canadian Airborne Biodiversity Observatory (CABO) project, which is funded by a Discovery Frontiers grant from Natural Sciences and Engineering Research Council of Canada (NSERC; Grant number 509190-2017). EL was also supported by a Discovery Grant from NSERC (Grant number RGPIN-2014-06106).

References

Aasen, H., Honkavaara, E., Lucieer, A., and Zarco-Tejada, P. 2018. Quantitative remote sensing at ultra-high resolution with uav spectroscopy: A review of sensor technology, measurement procedures, and data correction workflows. Remote Sensing **10**(7): 1091.

Arroyo-Mora, J.P., Kalacska, M., Inamdar, D., Soffer, R., Lucanus, O., Gorman, J., Naprstek, T., Schaaf, E.S., Ifimov, G., and Elmer, K. 2019. Implementation of a UAV–Hyperspectral Pushbroom Imager for Ecological Monitoring. Drones **3**(1): 12.

Asner, G.P. and Martin, R.E. 2008. Airborne spectranomics: mapping canopy chemical and taxonomic diversity in tropical forests. Frontiers in Ecology and the Environment **7**(5): 269-276.

Asner, G.P., Brodrick, P.G., Anderson, C.B., Vaughn, N., Knapp, D.E., and Martin, R.E. 2016. Progressive forest canopy water loss during the 2012–2015 California drought. Proceedings of the National Academy of Sciences **113**(2): E249-E255.

Asner, G.P., Martin, R.E., Knapp, D., Tupayachi, R., Anderson, C., Sinca, F., Vaughn, N., and Llactayo, W. 2017. Airborne laser-guided imaging spectroscopy to map forest trait diversity and guide conservation. Science **355**(6323): 385-389.

Asner, G.P., Martin, R.E., Knapp, D.E., Tupayachi, R., Anderson, C., Carranza, L., Martinez, P., Houcheime, M., Sinca, F., and Weiss, P. 2011. Spectroscopy of canopy chemicals in humid tropical forests. Remote Sensing of Environment **115**(12): 3587-3598.

Ayotte, J. and Laliberté, E. 2019. Measuring leaf carbon fractions with the ANKOM2000 Fiber Analyzer.

Ayotte, J., Guilbeault-Mayers, X., and Laliberté, E. 2019. Measuring CN content in leaf samples using Elementar Vario MICRO Cube. Available from https://www.protocols.io/view/measuring-cn-content-in-leaf-samples-using-element-udces2w.

Bates, D., Mächler, M., Bolker, B., and Walker, S. 2014. Fitting linear mixed-effects models using lme4. arXiv preprint arXiv:1406.5823.

Bush, A., Sollmann, R., Wilting, A., Bohmann, K., Cole, B., Balzter, H., Martius, C., Zlinszky, A., Calvignac-Spencer, S., and Cobbold, C.A. 2017. Connecting Earth observation to high-throughput biodiversity data. Nature Ecology & Evolution **1**(7): 0176.

Cavender-Bares, J., Gamon, J.A., Hobbie, S.E., Madritch, M.D., Meireles, J.E., Schweiger, A.K., and Townsend, P.A. 2017. Harnessing plant spectra to integrate the biodiversity sciences across biological and spatial scales. American Journal of Botany **104**(7): 966-969.

Charron, G., Robichaud-Courteau, T., La Vigne, H., Weintraub, S., Hill, A., Justice, D., Bélanger, N., and Lussier Desbiens, A. 2020. The DeLeaves: A UAV device for efficient tree canopy sampling. Journal of Unmanned Vehicle Systems. doi:10.1139/juvs-2020-0005.

Clark, M.L., Roberts, D.A., and Clark, D.B. 2005. Hyperspectral discrimination of tropical rain forest tree species at leaf to crown scales. Remote sensing of environment **96**(3-4): 375-398.

Curran, P.J. 1989. Remote sensing of foliar chemistry. Remote Sensing of Environment **30**(3): 271-278.

Curran, P.J., Dungan, J.L., and Peterson, D.L. 2001. Estimating the foliar biochemical concentration of leaves with reflectance spectrometry: testing the Kokaly and Clark methodologies. Remote Sensing of Environment **76**(3): 349-359.

Curtis, P.G., Slay, C.M., Harris, N.L., Tyukavina, A., and Hansen, M.C. 2018. Classifying drivers of global forest loss. Science **361**(6407): 1108-1111. doi:10.1126/science.aau3445.

Demmig-Adams, B. and Adams, W.W.I. 1996. The role of xanthophyll cycle carotenoids in the protection of photosynthesis. Trends in Plant science **1**(1): 21-26.

Draper, F.C., Baraloto, C., Brodrick, P.G., Phillips, O.L., Martinez, R.V., Honorio Coronado, E.N., Baker, T.R., Zárate Gómez, R., Amasifuen Guerra, C.A., and Flores, M. 2019. Imaging spectroscopy predicts variable distance decay across contrasting Amazonian tree communities. Journal of Ecology **107**(2): 696-710.

Ellsworth, D. and Reich, P.B. 1993. Canopy structure and vertical patterns of photosynthesis and related leaf traits in a deciduous forest. Oecologia **96**(2): 169-178.

Evans, J.R. and Seemann, J.R. 1989. The allocation of protein nitrogen in the photosynthetic apparatus: cost, consequences and control. *In* Photosynthesis. *Edited by* W.R. Briggs. Alan R. Liss Inc., New York. pp. 183–205.

Fassnacht, F.E., Latifi, H., Stereńczak, K., Modzelewska, A., Lefsky, M., Waser, L.T., Straub, C., and Ghosh, A. 2016. Review of studies on tree species classification from remotely sensed data. Remote Sensing of Environment **186**: 64-87.

Féret, J.-B. and Asner, G.P. 2014. Mapping tropical forest canopy diversity using high-fidelity imaging spectroscopy. Ecological Applications **24**(6): 1289-1296.

Foster, J.R. and Townsend, P.A. Linking hyperspectral imagery and forest inventories for forest assessment in the Central Appalachians. *In* Proceedings of the 14th Central Hardwood Conference. 2004.

Gamon, J., Penuelas, J., and Field, C. 1992. A narrow-waveband spectral index that tracks diurnal changes in photosynthetic efficiency. Remote Sensing of environment **41**(1): 35-44.

Gamon, J.A. 2015. Reviews and Syntheses: optical sampling of the flux tower footprint. Biogeosciences **12**: 4509–4523. doi:10.5194/bg-12-4509-2015.

Gamon, J.A. and Berry, J.A. 2012. Facultative and constitutive pigment effects on the Photochemical Reflectance Index (PRI) in sun and shade conifer needles. Israel Journal of Plant Sciences **60**(1-2): 85-95.

Gamon, J.A., Cheng, Y., Claudio, H., MacKinney, L., and Sims, D.A. 2006. A mobile tram system for systematic sampling of ecosystem optical properties. Remote Sensing of Environment **103**(3): 246-254. doi:http://dx.doi.org/10.1016/j.rse.2006.04.006.

Gates, D.M., Keegan, H.J., Schleter, J.C., and Weidner, V.R. 1965. Spectral properties of plants. Applied optics **4**(1): 11-20.

Green, R.O., Eastwood, M.L., Sarture, C.M., Chrien, T.G., Aronsson, M., Chippendale, B.J., Faust, J.A., Pavri, B.E., Chovit, C.J., and Solis, M. 1998. Imaging spectroscopy and the airborne visible/infrared imaging spectrometer (AVIRIS). Remote sensing of environment **65**(3): 227-248.

Guanter, L., Kaufmann, H., Segl, K., Foerster, S., Rogass, C., Chabrillat, S., Kuester, T., Hollstein, A., Rossner, G., and Chlebek, C. 2015. The EnMAP spaceborne imaging spectroscopy mission for earth observation. Remote Sensing **7**(7): 8830-8857.

Hart, S.P., Schreiber, S.J., and Levine, J.M. 2016. How variation between individuals affects species coexistence. Ecology letters **19**(8): 825-838.

Herrmann, I., Vosberg, S., Ravindran, P., Singh, A., Chang, H.-X., Chilvers, M., Conley, S., and Townsend, P. 2018. Leaf and Canopy Level Detection of Fusarium Virguliforme (Sudden Death Syndrome) in Soybean. Remote Sensing **10**(3): 426. Available from http://www.mdpi.com/2072-4292/10/3/426 [accessed.

Humphreys, A.M., Govaerts, R., Ficinski, S.Z., Nic Lughadha, E., and Vorontsova, M.S. 2019. Global dataset shows geography and life form predict modern plant extinction and rediscovery. Nature Ecology & Evolution **3**(7): 1043-1047. doi:10.1038/s41559-019-0906-2.

Iwasaki, A., Ohgi, N., Tanii, J., Kawashima, T., and Inada, H. Hyperspectral Imager Suite (HISUI) -Japanese hyper-multi spectral radiometer. *In* 2011 IEEE International Geoscience and Remote Sensing Symposium. 24-29 July 2011 2011. pp. 1025-1028.

Jetz, W., Cavender-Bares, J., Pavlick, R., Schimel, D., Davis, F.W., Asner, G.P., Guralnick, R., Kattge, J., Latimer, A.M., and Moorcroft, P. 2016. Monitoring plant functional diversity from space. Nature plants **2**: 16024.

Knipling, E.B. 1970. Physical and physiological basis for the reflectance of visible and near-infrared radiation from vegetation. Remote sensing of environment **1**(3): 155-159.

Kokaly, R.F. and Clark, R.N. 1999. Spectroscopic determination of leaf biochemistry using band-depth analysis of absorption features and stepwise multiple linear regression. Remote Sensing of Environment **67**(3): 267-287.

Laliberté, E. 2018. Measuring specific leaf area and water content. Available from https://www.protocols.io/view/measuring-specific-leaf-area-and-water-content-p3tdqnn.

Laliberté, E. and Soffer, R. 2018. Measuring spectral reflectance and transmittance (350-2500 nm) of large leaves using the Spectra Vista Corporation (SVC) DC-R/T Integrating Sphere. Available from https://www.protocols.io/view/measuring-spectral-reflectance-and-transmittance-3-p8pdrvn.

Laliberté, E., Schweiger, A.K., and Legendre, P. 2019. Partitioning plant spectral diversity into alpha and beta components. Ecology letters.

Laughlin, D.C. 2014. Applying trait-based models to achieve functional targets for theory-driven ecological restoration. Ecology letters **17**(7): 771-784.

Lavorel, S. and Garnier, É. 2002. Predicting changes in community composition and ecosystem functioning from plant traits: revisiting the Holy Grail. Functional ecology **16**(5): 545-556.

Lichtenthaler, H., Buschmann, C., Döll, M., Fietz, H.-J., Bach, T., Kozel, U., Meier, D., and Rahmsdorf, U. 1981. Photosynthetic activity, chloroplast ultrastructure, and leaf characteristics of high-light and low-light plants and of sun and shade leaves. Photosynthesis research **2**(2): 115-141.

Lopatin, J., Fassnacht, F.E., Kattenborn, T., and Schmidtlein, S. 2017. Mapping plant species in mixed grassland communities using close range imaging spectroscopy. Remote Sensing of Environment **201**: 12-23. doi:https://doi.org/10.1016/j.rse.2017.08.031.

Madritch, M.D., Kingdon, C.C., Singh, A., Mock, K.E., Lindroth, R.L., and Townsend, P.A. 2014. Imaging spectroscopy links aspen genotype with below-ground processes at landscape scales. Philosophical Transactions of the Royal Society of London B: Biological Sciences **369**(1643): 20130194.

Martens, H. 2001. Reliable and relevant modelling of real world data: a personal account of the development of PLS regression. Chemometrics and intelligent laboratory systems **58**(2): 85-95.

Maschler, J., Atzberger, C., and Immitzer, M. 2018. Individual tree crown segmentation and classification of 13 tree species using Airborne hyperspectral data. Remote Sensing **10**(8): 1218.

McGill, B.J., Enquist, B.J., Weiher, E., and Westoby, M. 2006. Rebuilding community ecology from functional traits. Trends in Ecology & Evolution **21**(4): 178-185.

National Academies of Sciences, E. and Medicine. 2018. Thriving on Our Changing Planet: A Decadal Strategy for Earth Observation from Space. The National Academies Press, Washington, DC.

Niinemets, Ü. 2007. Photosynthesis and resource distribution through plant canopies. Plant, Cell & Environment **30**(9): 1052-1071.

Ollinger, S.V. 2011. Sources of variability in canopy reflectance and the convergent properties of plants. New Phytologist **189**(2): 375-394. doi:10.1111/j.1469-8137.2010.03536.x.

Osnas, J.L., Lichstein, J.W., Reich, P.B., and Pacala, S.W. 2013. Global leaf trait relationships: mass, area, and the leaf economics spectrum. Science **340**(6133): 741-744.

Palmer, M.W., Earls, P.G., Hoagland, B.W., White, P.S., and Wohlgemuth, T. 2002. Quantitative tools for perfecting species lists. Environmetrics: The official journal of the International Environmetrics Society **13**(2): 121-137.

Perez-Harguindeguy, N., Diaz, S., Garnier, E., Lavorel, S., Poorter, H., Jaureguiberry, P., and Bret-Harte, M. 2013. New handbook for standardised measurement of plant functional traits worldwide. Australian Journal **800**: 167-234.

Pontius, J., Hallett, R., and Martin, M. 2005. Using AVIRIS to assess hemlock abundance and early decline in the Catskills, New York. Remote Sensing of Environment **97**(2): 163-173.

R Core Team. 2019. R: A language and environment for statistical computing. R Foundation for Statistical Computing, Vienna.

Reich, P.B., Walters, M.B., and Ellsworth, D.S. 1997. From tropics to tundra: global convergence in plant functioning. Proceedings of the National Academy of Sciences **94**(25): 13730-13734.

Rocchini, D., Balkenhol, N., Carter, G.A., Foody, G.M., Gillespie, T.W., He, K.S., Kark, S., Levin, N., Lucas, K., and Luoto, M. 2010. Remotely sensed spectral heterogeneity as a proxy of species diversity: recent advances and open challenges. Ecological Informatics **5**(5): 318-329.

Rockström, J., Steffen, W., Noone, K., Persson, Å., Chapin III, F.S., Lambin, E.F., Lenton, T.M., Scheffer, M., Folke, C., and Schellnhuber, H.J. 2009. A safe operating space for humanity. Nature **461**(7263): 472.

Rogers, A., Medlyn, B.E., Dukes, J.S., Bonan, G., Von Caemmerer, S., Dietze, M.C., Kattge, J., Leakey, A.D., Mercado, L.M., and Niinemets, Ü. 2017. A roadmap for improving the representation of photosynthesis in Earth system models. New Phytologist **213**(1): 22-42.

Schaepman, M.E., Ustin, S.L., Plaza, A.J., Painter, T.H., Verrelst, J., and Liang, S. 2009. Earth system science related imaging spectroscopy-An assessment. Remote Sensing of Environment **113**(SUPPL. 1): S123-S137. Available from http://www.scopus.com/inward/record.url?eid=2-s2.0-67650270441&partnerID=40&md5=874f5734a40a51f3a49da7130d7b6db5 [accessed.

Schaepman, M.E., Jehle, M., Hueni, A., D'Odorico, P., Damm, A., Weyermann, J., Schneider, F.D., Laurent, V., Popp, C., Seidel, F.C., Lenhard, K., Gege, P., Küchler, C., Brazile, J., Kohler, P., De Vos, L., Meuleman, K., Meynart, R., Schläpfer, D., Kneubühler, M., and Itten, K.I. 2015. Advanced radiometry measurements and Earth science applications with the Airborne Prism Experiment (APEX). Remote Sensing of Environment **158**: 207-219. doi:https://doi.org/10.1016/j.rse.2014.11.014.

Schimel, D.S., Asner, G.P., and Moorcroft, P. 2013. Observing changing ecological diversity in the Anthropocene. Frontiers in Ecology and the Environment **11**(3): 129-137.

Schweiger, A.K. and Laliberté, E. 2019. Spectral processing protocol.

Schweiger, A.K., Schütz, M., Risch, A.C., Kneubühler, M., Haller, R., and Schaepman, M.E. 2017. How to predict plant functional types using imaging spectroscopy: linking vegetation community traits, plant functional types and spectral response. Methods in Ecology and Evolution **8**(1): 86-95.

Schweiger, A.K., Cavender-Bares, J., Townsend, P.A., Hobbie, S.E., Madritch, M.D., Wang, R., Tilman, D., and Gamon, J.A. 2018. Plant spectral diversity integrates functional and phylogenetic components of biodiversity and predicts ecosystem function. Nature Ecology & Evolution. doi:10.1038/s41559-018-0551-1.

Serbin, S.P., Wu, J., Ely, K.S., Kruger, E.L., Townsend, P.A., Meng, R., Wolfe, B.T., Chlus, A., Wang, Z., and Rogers, A. 2019. From the Arctic to the tropics: multi-biome prediction of leaf mass per area using leaf reflectance. New Phytologist.

Shipley, B., Vile, D., Garnier, E., Wright, I., and Poorter, H. 2005. Functional linkages between leaf traits and net photosynthetic rate: reconciling empirical and mechanistic models. Functional ecology **19**(4): 602-615.

Shipley, B., De Bello, F., Cornelissen, J.H.C., Laliberté, E., Laughlin, D.C., and Reich, P.B. 2016. Reinforcing loose foundation stones in trait-based plant ecology. Oecologia **180**(4): 923-931.

Singh, A., Ganapathysubramanian, B., Singh, A.K., and Sarkar, S. 2016. Machine learning for high-throughput stress phenotyping in plants. Trends in plant science **21**(2): 110-124.

Singh, A., Serbin, S.P., McNeil, B.E., Kingdon, C.C., and Townsend, P.A. 2015. Imaging spectroscopy algorithms for mapping canopy foliar chemical and morphological traits and their uncertainties. Ecological Applications **25**(8): 2180-2197.

Slaton, M.R., Raymond Hunt Jr, E., and Smith, W.K. 2001. Estimating near-infrared leaf reflectance from leaf structural characteristics. American Journal of Botany **88**(2): 278-284.

Stavros, E.N., Schimel, D., Pavlick, R., Serbin, S., Swann, A., Duncanson, L., Fisher, J.B., Fassnacht, F., Ustin, S., Dubayah, R., Schweiger, A.K., and Wenneberg, P. 2017. ISS Observations Offer Insights Into Plant Function. Nature Ecology and Evolution **1**(BNL--113983-2017-JA).

Turner, W. 2014. Sensing biodiversity. Science **346**(6207): 301-302.

Ustin, S.L. and Gamon, J.A. 2010. Remote sensing of plant functional types. New Phytologist **186**(4): 795-816. Available from http://www.scopus.com/inward/record.url?eid=2-s2.0-77953955155&partnerID=40&md5=e31a579227952083fc671714bf921c0d [accessed.

Ustin, S.L., Roberts, D.A., Gamon, J.A., Asner, G.P., and Green, R.O. 2004. Using imaging spectroscopy to study ecosystem processes and properties. BioScience **54**(6): 523-534.

Available from http://www.scopus.com/inward/record.url?eid=2-s2.0-2942528742&partnerID=40&md5=2836f861398530378aa58f5bc04d4320 [accessed.

Ustin, S.L., Gitelson, A.A., Jacquemoud, S., Schaepman, M.E., Asner, G.P., Gamon, J.A., and Zarco-Tejada, P. 2009. Retrieval of foliar information about plant pigment systems from high resolution spectroscopy. Remote Sensing of Environment **113**: S67-S77.

Valladares, F. and Niinemets, Ü. 2008. Shade tolerance, a key plant feature of complex nature and consequences. Annual Review of Ecology, Evolution, and Systematics **39**: 237-257.

Vile, D., Garnier, E., Shipley, B., Laurent, G., Navas, M.-L., Roumet, C., Lavorel, S., Diaz, S., Hodgson, J.G., and Lloret, F. 2005. Specific leaf area and dry matter content estimate thickness in laminar leaves. Annals of botany **96**(6): 1129-1136.

Violle, C., Reich, P.B., Pacala, S.W., Enquist, B.J., and Kattge, J. 2014. The emergence and promise of functional biogeography. Proceedings of the National Academy of Sciences **111**(38): 13690-13696.

Vogelman, T.C., Nishio, J.N., and Smith, W.K. 1996. Leaves and light capture: Light propagation and gradients of carbon fixation within leaves. Trends in Plant Science **1**(2): 65-70. doi:https://doi.org/10.1016/S1360-1385(96)80031-8.

Wang, R. and Gamon, J.A. 2019. Remote sensing of terrestrial plant biodiversity. Remote Sensing of Environment **231**: 111218. doi:https://doi.org/10.1016/j.rse.2019.111218.

Wang, R., Gamon, J.A., Cavender-Bares, J., Townsend, P.A., and Zygielbaum, A.I. 2018. The spatial sensitivity of the spectral diversity–biodiversity relationship: an experimental test in a prairie grassland. Ecological Applications **28**(2): 541-556.

Wang, Z., Townsend, P.A., Schweiger, A.K., Couture, J.J., Singh, A., Hobbie, S.E., and Cavender-Bares, J. 2019. Mapping foliar functional traits and their uncertainties across three years in a grassland experiment. Remote sensing of environment **221**: 405-416.

Wold, S., Martens, H., and Wold, H. The multivariate calibration problem in chemistry solved by the PLS method. *In* Matrix pencils, Lecture Notes in Mathematics. 1983. *Edited by* A. Ruhe and B. Kagstrom. Springer, Heidelberg. pp. 286-293.

Wright, I.J., Reich, P.B., Westoby, M., Ackerly, D.D., Baruch, Z., Bongers, F., Cavender-Bares, J., Chapin, T., Cornelissen, J.H., and Diemer, M. 2004. The worldwide leaf economics spectrum. Nature **428**(6985): 821-827.

Youngentob, K.N., Zdenek, C., and Gorsel, E. 2016. A simple and effective method to collect leaves and seeds from tall trees. Methods in Ecology and Evolution **7**(9): 1119-1123. doi:doi:10.1111/2041-210X.12554.

Tables

Table 1. Differences in chemical and structural traits, and the photochemical reflectance index (PRI) between sunlit sugar maples leaves from the top and side of the crown; we rejected the null model (M0) of no effect of sampling position on foliar traits and PRI when the model including an effect of sampling position (M1) was at least four times (likelihood ratio > 4) more likely than M0 (highlighted in bold).

Trait	Model	df	Likelihood ratio	P value
Leaf thickness (µm)	**M1**	**4**	**14.44**	**0.0001**
Leaf mass per area (g m^{-2})	**M1**	**4**	**14.34**	**0.0002**
Equivalent water thickness (µm)	**M1**	**4**	**10.91**	**0.0010**
Relative water content (%)	**M1**	**4**	**9.94**	**0.0016**
Leaf water content (mg g^{-1})	M0	3	0.60	0.4378
Leaf dry matter content (mg g^{-1})	M0	3	0.60	0.4378
Nitrogen (mg cm^{-2})	**M1**	**4**	**14.89**	**0.0001**
Nitrogen (%)	M0	3	1.49	0.2216
Carbon (mg cm^{-2})	**M1**	**4**	**13.20**	**0.0003**
Carbon (%)	M0	3	0.25	0.6146
Nonstructural carbohydrates (mg cm^{-2})	**M1**	**4**	**14.15**	**0.0002**
Nonstructural carbohydrates (%)	M0	3	2.49	0.1149
Hemicellulose (mg cm^{-2})	M0	3	0.61	0.4362
Hemicellulose (%)	M0	3	0.77	0.3793
Cellulose (mg cm^{-2})	**M1**	**4**	**8.73**	**0.0031**
Cellulose (%)	**M1**	**4**	**9.72**	**0.0018**
Lignin (mg cm^{-2})	**M1**	**4**	**13.27**	**0.0003**
Lignin (%)	M0	3	0.16	0.6865
Photochemical reflectance index (PRI)	**M1**	**4**	**4.31**	**0.0380**

Figures

Fig. 1. Sampling of sunlit leaves (A) with a pole pruner from the side of the crown, and (B) with an Unmanned Aerial System (UAS) and the DeLeaves twig-sampling tool from the top of the crown.

Fig. 2. Sunlit sugar maple leaves from the top of the crown had higher (A) leaf mass per area (LMA, g m^{-2}), (B) leaf thickness (µm), (C) nitrogen content per area (mg cm^{-2}) and (D) equivalent water thickness (µm), but lower (E) relative water content (RWC, %), and (F) cellulose content per mass (%) than sunlit leaves from the side of the crown. Plots show means +/- standard deviations; dashed lines connect samples from the same trees; for statistics see Table 1.

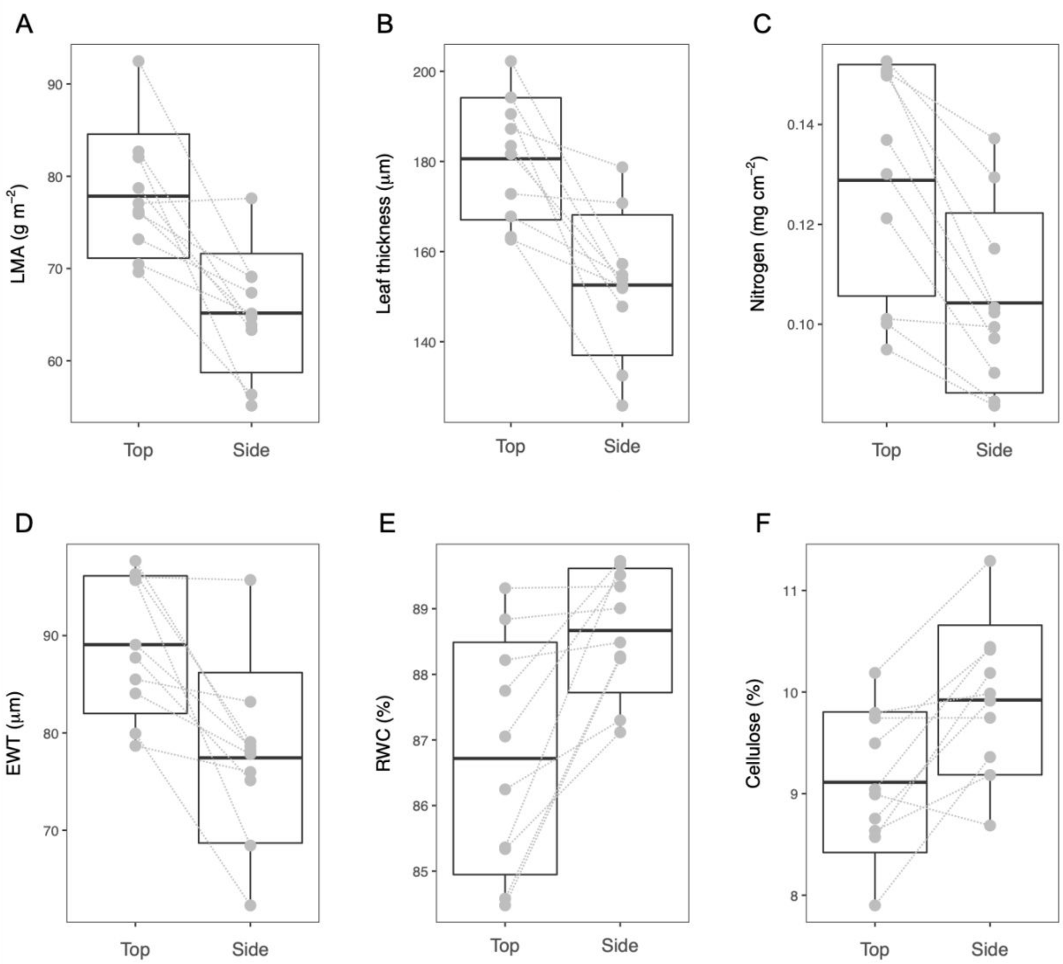

Fig. 3. Differences in (A) absorbance, and (B) absolute reflectance (bottom) and transmittance (top) between sunlit sugar maple leaves sampled from the top (red) and side (blue) of the crown. Wavelength regions that were at least four times more likely to be affected by sampling position than not affected are shaded in grey; red and blue lines indicate mean spectra, red and blue shaded areas 95% of the sample distribution.